Wind Energy

WIND ENERGY
Wind Energ. 2016; **19**:1439–1452
Published online 30 September 2015 in Wiley Online Library (wileyonlinelibrary.com). DOI: 10.1002/we.1929

RESEARCH ARTICLE

A new formulation for rotor equivalent wind speed for wind resource assessment and wind power forecasting

Aditya Choukulkar[1], Yelena Pichugina[1], Christopher T. M. Clack[1], Ronald Calhoun[2], Robert Banta[3], Alan Brewer[3] and Michael Hardesty[1]

[1] Cooperative Institute for Research in Environmental Sciences, Boulder, Colorado, USA
[2] Environmental Remote Sensing Group, Arizona State University, Tempe, Arizona, USA
[3] Chemical Sciences Division, National Oceanic and Atmospheric Administration, Boulder, Colorado, USA

ABSTRACT

The spurt of growth in the wind energy industry has led to the development of many new technologies to study this energy resource and improve the efficiency of wind turbines. One of the key factors in wind farm characterization is the prediction of power output of the wind farm that is a strong function of the turbulence in the wind speed and direction. A new formulation for calculating the expected power from a wind turbine in the presence of wind shear, turbulence, directional shear and direction fluctuations is presented. It is observed that wind shear, directional shear and direction fluctuations reduce the power producing capability, while turbulent intensity increases it. However, there is a complicated superposition of these effects that alters the characteristics of the power estimate that indicates the need for the new formulation. Data from two field experiments is used to estimate the wind power using the new formulation, and results are compared to previous formulations. Comparison of the estimates of available power from the new formulation is not compared to actual power outputs and will be a subject of future work. © 2015 The Authors. *Wind Energy* published by John Wiley & Sons, Ltd.

KEYWORDS
wind energy; equivalent wind speed; wind power calculation; Doppler lidar; wind resource assessment; wind power forecasting

Correspondence
A. Choukulkar, Cooperative Institute for Research in Environmental Sciences, University of Colorado, Boulder, Colorado 80305, USA.
E-mail: aditya.choukulkar@noaa.gov

Received 20 October 2014; Revised 18 August 2015; Accepted 23 August 2015

1. INTRODUCTION

The recent surge in the technological advances in the field of wind energy has seen development of turbines capable of producing power in the multi-MW range. Advances in wind turbine technology have resulted in wind turbines with hub-heights routinely over 100 m and rotor diameters reaching as high as 160 m (e.g. the Vestas V164 unveiled in 2014). With increased size and power capacity of wind turbines, come concerns of accurately predicting the power output from these turbines. Traditionally, wind measurements have been carried out using meteorological towers which provide point measurements at hub heights. With the increase in rotor swept area and hub heights, the impact of wind shear and turbulence intensity become increasingly relevant, and point measurements from meteorological towers no longer are good representations of the wind interacting with the turbine (e.g. Sumner *et al.*[1], Wagner *et al.*[2] and Wharton and Lundquist[3]).

Direct implications of these developments are in the areas of power forecasting and wind turbine control. No longer is it enough to measure/predict wind speed at hub-height in order to estimate wind power production. In addition to the variability in wind speed and direction with height, the turbulence parameters such as fluctuations of velocity components and direction fluctuations are important for determining the power availability. The effect of wind speed turbulence on wind power production has been a subject of considerable research, e.g. Elliot and Cadogan[4] demonstrated the influence of wind shear and turbulence on wind turbine power curves. Wagner *et al.*[2] showed that significant error in power measurement

could result if the effect of wind shear was ignored and demonstrated the use of equivalent wind speed method for power curve measurement.

Wind speed fluctuations are often accompanied by fluctuations in wind direction. The power output is calculated assuming the wind interacts with the rotor parallel to its axis. Misalignment of the wind direction with the rotor axis can significantly reduce the power output. Akhmatov[5] describes the influence of wind direction on wind power fluctuations. Pedersen[6] using the 3D actuator disk model showed that the power output is related to the yaw angle error through a $\cos^2$ relationship. But these studies do not quantify the effect of fluctuations in the wind direction. In addition, it is not uncommon to find shear in wind direction to accompany shear in wind speed across the rotor swept area. Therefore, the combined effects of the shear in wind direction and wind speed need to be considered for accurate assessment of the wind power output. In the present paper, theoretical formulations will be presented that take into account the effects of wind speed direction fluctuations, wind shear, wind speed turbulence and directional shear on wind power output. The rest of the paper is structured as follows. In section 2, we will derive an expression that accounts for turbulence in velocity and direction as well as shear in velocity and direction. From this, an expression for equivalent wind speed will be developed. In section 3 the effect of the above parameters on wind power production will be quantified for ideal cases. Section 4 will discuss power calculations using lidar data in flat homogenous terrain and complex terrain, and Section 5 outlines the conclusions and future work.

2. NEW EQUIVALENT WIND SPEED FORMULATION

The effect of wind shear and wind direction on power output of wind turbines has been evaluated independently (e.g. Wagner *et al.*[2], Kaiser *et al.*[7] and Antoniou *et al.*[8]). However, these effects do not occur in isolation. Therefore, the following formulation will attempt to quantify their combined effect. To start off, the power available in the wind can be expressed in the form of wind power flux or kinetic energy flux[2] defined as:

$$P(t) = \frac{1}{2}\rho C_P A U^3(t) \tag{1}$$

where ρ is the density of air, C_P is the coefficient of power, A is the rotor swept area and $U(t)$ is the instantaneous wind speed. Equation (1) assumes that the wind hits the wind turbine parallel to the axis and that the wind is uniform over the rotor swept area. If the wind interacts with the turbine at an angle φ, as shown in Figure 1, then to account for the possibility of azimuthal angle variations in the airflow, we re-write the equation (1) as:

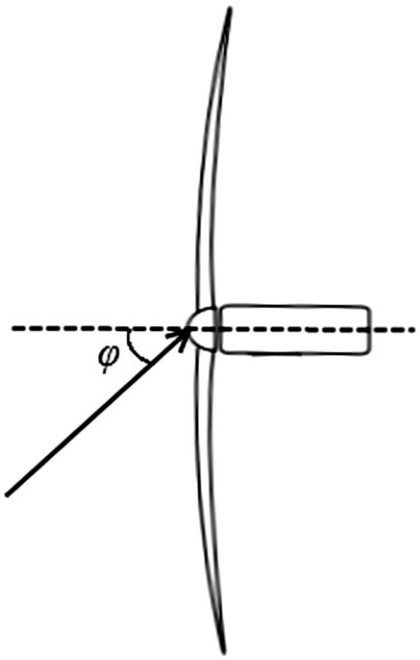

Figure 1. Top view of a wind turbine rotor showing the wind hitting the rotor at an angle φ in the horizontal plane.

$$P(t) = \frac{1}{2}\rho C_P A[U(t)\cos\varphi(t)]^3 \tag{2}$$

where $\varphi(t)$ is the angle of the wind to the turbine axis. Usually the quantity of interest is a temporal average of the power. In order to derive an expression for temporally averaged power, we perform a Reynold's decomposition:[9]

$$U(t) = \overline{U}(t) + u'(t) \quad \text{and} \quad \varphi(t) = \overline{\varphi}(t) + \varphi'(t) \tag{3}$$

where, $\overline{U}(t)$ and $\overline{\varphi}(t)$ are the temporal means of the wind speed and wind direction respectively and $u'(t)$ and $\varphi'(t)$ are perturbations or fluctuations about their respective means. Hereafter, for simplicity of notation, $\overline{U}(t)$, $u'(t)$, $\overline{\varphi}(t)$ and $\varphi'(t)$ will be written as $\overline{U}$, u', $\overline{\varphi}$ and φ' respectively. Substituting equation (3) into equation (2) and performing a Taylor's expansion we find:

$$\begin{aligned} P(t) &= \frac{1}{2}\rho C_P A\left[\overline{U} + u'\right]^3[\cos(\overline{\varphi} + \varphi')]^3 \\ &\approx \frac{1}{2}\rho C_P A\left[\overline{U} + u'\right]^3\left[1 - \frac{(\overline{\varphi} + \varphi')^2}{2} + \ldots\right]^3 \\ &\approx \frac{1}{2}\rho C_P A\overline{U}^3\left[1 + u'\overline{U}\right]^3\left[1 - \frac{\overline{\varphi}^2}{2}\left(1 + \frac{\varphi'}{\overline{\varphi}}\right)^2 + \ldots\right]^3 \\ &\approx \frac{1}{2}\rho C_P A\overline{U}^3\left[1 + 3\frac{u'}{\overline{U}} + \frac{6}{2!}\left(\frac{u'}{\overline{U}}\right)^2 + \ldots\right]\left[1 - \frac{\overline{\varphi}^2}{2}\left(1 + 2\frac{\varphi'}{\overline{\varphi}} + \frac{\varphi'^2}{\overline{\varphi}^2}\right) + \ldots\right]^3 \end{aligned} \tag{4}$$

It is assumed that the higher order terms can be neglected. Now performing a temporal average of the above equation, $\overline{u'}$ and $\overline{\varphi'}$ go to zero and we have:

$$\overline{P} = \frac{1}{2}\rho C_P A\overline{U}^3\left[1 + 3\left(\frac{\sigma_u}{\overline{U}}\right)^2\right]\left[1 - \frac{\overline{\varphi}^2}{2} - \frac{\sigma_\varphi^2}{2}\right]^3 \tag{5}$$

where σ_u^2 is the variance of wind speed and σ_φ^2 is the variance of direction. From equation (5) we can write the turbulent equivalent wind speed as:

$$\overline{U}_T = \overline{U} \times \sqrt[3]{\left[1 + 3\left(\frac{\sigma_u}{\overline{U}}\right)^2\right]\left[1 - \frac{\overline{\varphi}^2}{2} - \frac{\sigma_\varphi^2}{2}\right]^3} \tag{6}$$

Equation (6) captures the effect of turbulence intensity, wind direction shear and direction fluctuations at one height level. However, as explained in Wagner *et al.*[2], these effects can vary over the rotor swept area and need to be weighted as a function of height. This is achieved by substituting equation (6) into the equivalent wind speed formulation proposed by Wagner *et al.*[2] (re-written in equation (7) below) that accounts for velocity change as a function of height. Substituting the turbulent equivalent wind speed, given by equation (6), into the shear equivalent wind speed we get:

$$\overline{U}_{eq} = \sqrt[3]{\frac{1}{A}\sum_{i=1}^{N}\overline{U}_{Ti}^3 A_i} = \sqrt[3]{\frac{1}{A}\sum_{i=1}^{N}\overline{U}_i^3\left[1 + 3\left(\frac{\sigma_{ui}}{\overline{U}_i}\right)^2\right]\left[1 - \frac{\overline{\varphi}_i^2}{2} - \frac{\sigma_{\varphi i}^2}{2}\right]^3 A_i} \tag{7}$$

where σ_{ui}^2 is the variance of velocity fluctuations at i-th level, φ_i is the angle of the wind with respect to the rotor axis at i-th level, $\overline{U}_i$ is the wind speed at the i-th level and $\sigma_{\varphi i}^2$ is the direction fluctuations at the i-th level.

Therefore the equivalent wind power content is given by:

$$\overline{P}_{eq} = \frac{1}{2}\rho C_P\sum_{i=1}^{N}\overline{U}_i^3\left(1 + 3\left(\frac{\sigma_{ui}}{\overline{U}_i}\right)^2\right)\left[1 - \frac{\overline{\varphi}_i^2}{2} - \frac{\sigma_{\varphi i}^2}{2}\right]^3 A_i \tag{8}$$

In the derivation of equation (8), it was assumed that perturbations in density are negligible. It was further assumed that the efficiency of a turbine is unaltered by the shear and turbulence, and hence the same C_p is used in equations (1), (2), (4), (5) and (8).

3. QUANTIFYING THE IMPACT OF TURBULENCE ON WIND POWER

From the equations derived in Section 2, it is possible to quantify the effect of turbulence and direction fluctuations on available wind power content. The available wind power content is strongly correlated with the wind power produced by the turbines and hence gives a reasonable estimate of the expected turbine performance in those conditions. Based on typical values of wind and direction shear as well as turbulence intensity,[3] the variations in available wind power content are estimated using equation (8). These variations are presented in Figure 2. For the power calculations presented here, we assume a wind turbine with hub height of 80 m and rotor diameter of 100 m. We arbitrarily assigned a hub-height wind speed of 10 m s^{-1}, and the power calculations for various conditions are normalized using this base condition.

As seen from Figure 2a, negative values of shear exponent increase available power, while positive values of shear exponent reduce available power (the minima is at $\alpha = 0.45$). It should be noted that this minima would change depending on the rotor diameter. Figure 2b shows that, theoretically, higher values of turbulence intensity increase the energy content of the wind. However when it comes to actual power production by the wind turbine, various studies (e.g. Akhmatov[5] and Tindal *et al.*[10]) have shown that turbulence intensity increases power production at lower wind speeds and reduces power production near the rated wind speeds. This shows one of the limitations of the formulation presented here. Therefore all the results presented here, especially effects of direction shear and direction fluctuations, need to be verified experimentally to determine the accuracy of this formulation. Figures 2c and 2d show that wind direction shear and direction fluctuations reduce the available wind power content. It should be noted that the range of values for the various parameters used to produce Figures 2 and 3 might extend beyond what is typically observed. This was done to demonstrate the theoretical response of available power based on the formulation presented in equation (8). Further studies are required to determine the expected range of values for these parameters and compare the theoretical response to actual power production.

Since, these four effects do not occur individually, but occur in combination, studying the combined effects of these parameters is essential to understand the variability in available wind power. Figure 3 shows the variation of wind power

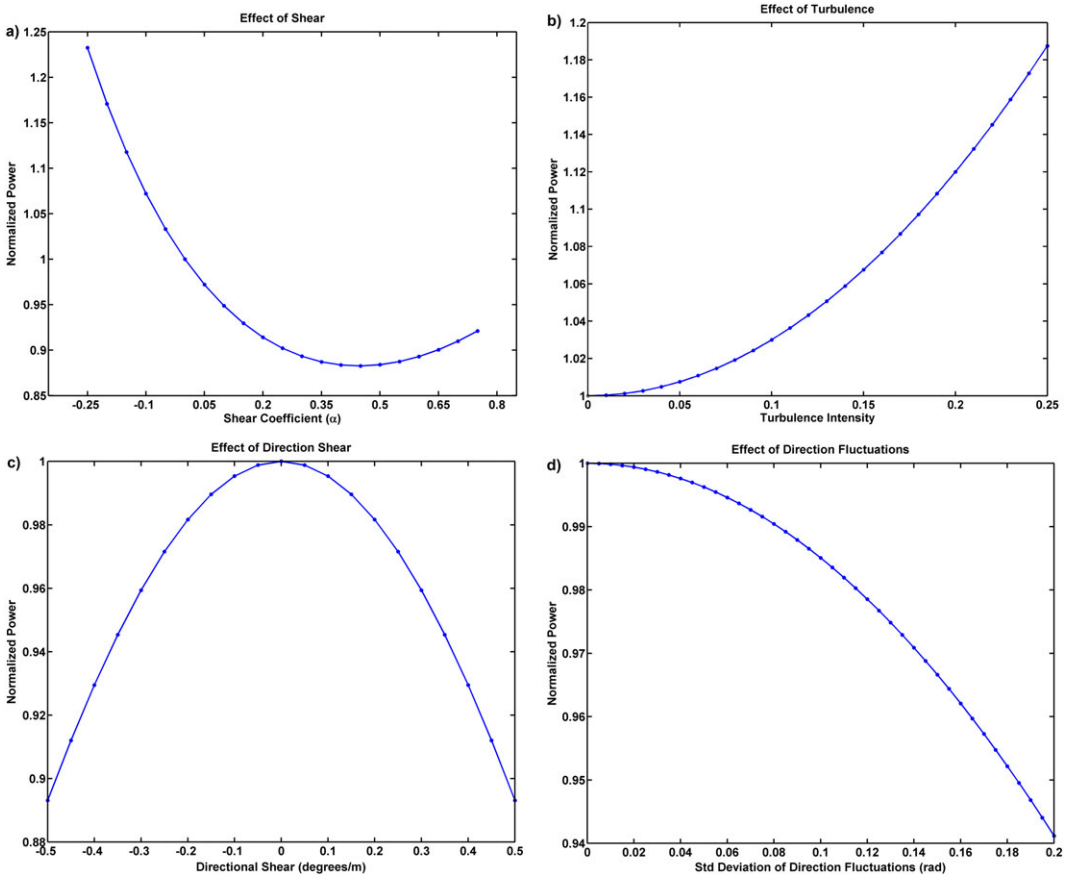

Figure 2. Modeling the theoretical effect of turbulence on available wind power content using equation (8). The wind power content is normalized with respect to the mean value in the absence of turbulence or shear. (a) Theoretical impact of wind speed shear. (b) Theoretical impact of turbulence intensity. (c) Theoretical impact of direction shear. (d) Theoretical impact of directional fluctuations.

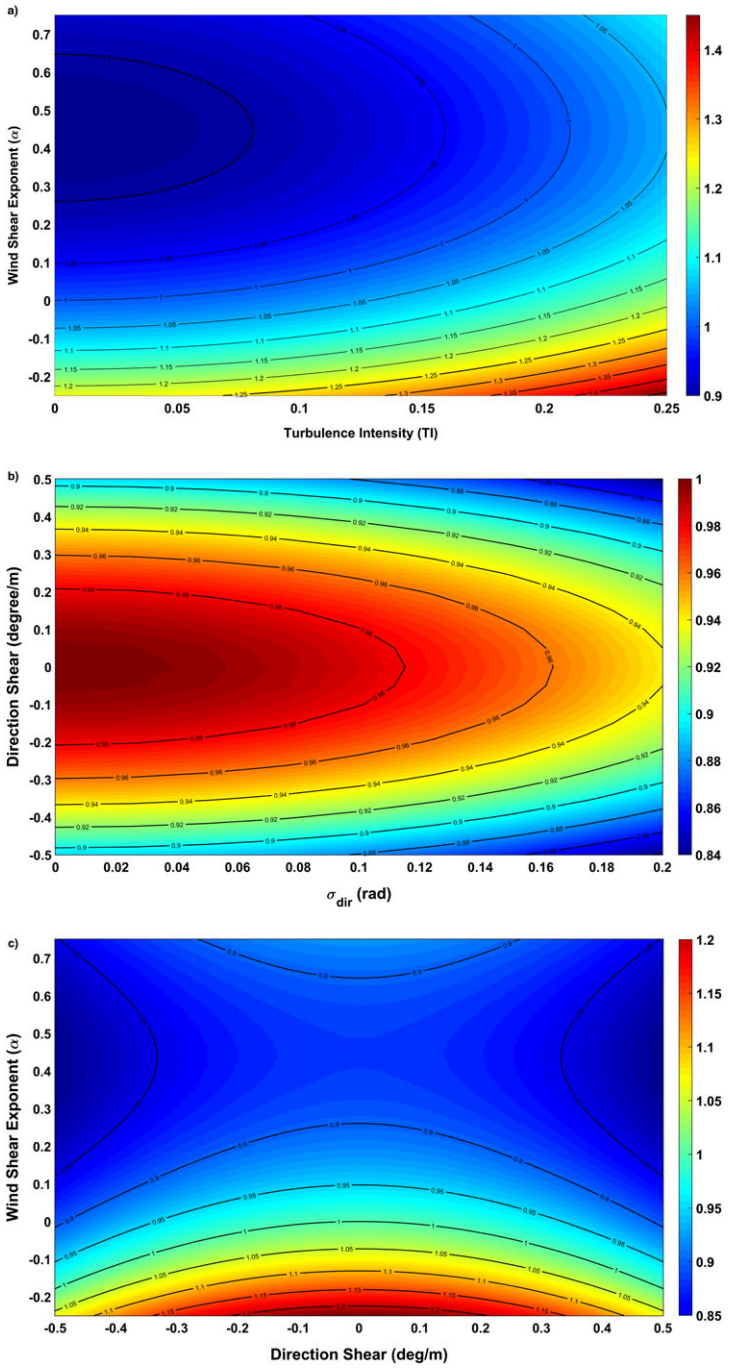

Figure 3. Combined effects of turbulence parameters on available wind power content. The wind power content is normalized with respect to the mean value in the absence of turbulence or shear and its magnitude is represented by the colors. (a) Combined effect of wind speed shear and turbulence intensity. (b) Combined effect of directional shear and direction fluctuations. (c) Combined effect of wind speed shear and directional shear.

content because of the combined effects of various turbulence parameters. It can be seen that the combined influence of turbulence and wind speed shear can produce deficits in available power up to 10%. And, wind direction shear and direction fluctuations can introduce deficits in available power of up to 14%. It is also observed from Figure 3c that wind speed shear and wind direction shear, which can result in available power deficits of ~15% or higher, are the main contributors to variations in available wind power.

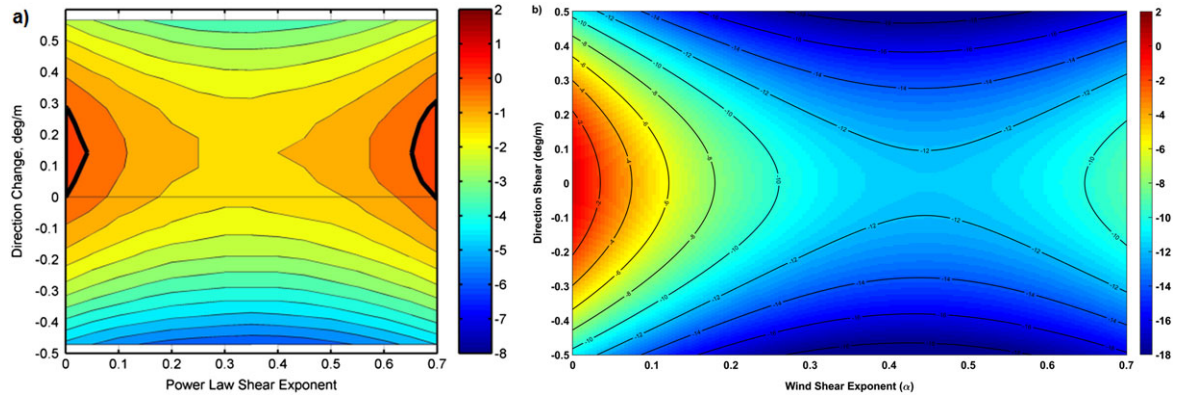

Figure 4. Comparison of combined effect of wind speed shear and wind direction shear. (a) Result from FAST simulation published in Walter.[11] Image reproduced here with permission of author. (b) Result from the new equivalent wind formulation (equation (8)). In both figures, the magnitude of color represents percentage change compared to value in absence of wind and direction shear.

The estimates for change in power because of wind shear and direction shear are compared with those presented by Walter[11] using the National Renewable Energy (NREL) FAST software in Figure 4 (see Figure 55 in Walter[11]). It is observed that the two analyses show a similar trend in power variation with two important differences. First, the results from Walter[11] show that effect of direction shear is not symmetric about zero (see Walter[11] for details on this), and the second is that the reduction in power estimated by the analytical formulation (equation (8)) is significantly higher. It should be noted that some differences are expected as using equation (8) we estimate the differences in available energy in the wind given the presence of wind and direction shear while the results from Walter[11] show differences in expected power production in presence of wind and direction shear as estimated by the FAST software which models the turbine response for a given inflow condition. That is, Figure 4(a) can be thought as modeled turbine response to difference in available energy shown in Figure 4(b). It is clear that there could be limitations to what the formulation presented here can predict about power production. However, estimates of available energy predicted using this formulation could still be quite useful for applications such as wind resources assessment and wind power forecasting especially if the correlations between available energy and actual power production is properly understood. Therefore it is clear that experimental evaluation of these effects is necessary to understand the actual influence of these variables on power production and determine the usefulness of this formulation.

4. POWER CALCULATIONS USING LIDAR DATA

Remote sensing instruments such as Doppler lidars can provide high temporal and spatial resolution measurements to compute mean profiles of wind speed and direction with a vertical binning as low as 1 m (see Pichugina *et al.*[12]). In the present section, the new formulation of the equivalent wind along with measurements from the High Resolution Doppler lidar (HRDL) developed at the National Oceanic and Atmospheric Administration (NOAA), as described in Grund *et al.*[13], is used to study of the effects of wind speed and direction shear on available wind power. The HRDL can provide measurements with 30 m range resolution either through fixed elevation horizontal slice scans (Plan Position Indicator—PPI) or fixed azimuth vertical slice scans (Range Height Indicator—RHI). The HRDL can produce data rich measurements in horizontal and vertical planes over a wind farm site allowing identification of fluid dynamic processes occurring over a wide range of scales (see, e.g. Pichugina *et al.*[12] and Banta *et al.*[14]).

Lidar data collected during two field deployments will be used to study the new formulation for wind power availability. The first field experiment called Lamar Low Level Jet Project (a wind energy experiment in southeast Colorado) was conducted in September 2003 at a high plains location south of the town Lamar.[15] The 2 week lidar deployment was a part of the ongoing 2 year experiment conducted at this site by the National Renewable Energy Laboratory (NREL) prior to the siting a wind farm (about 100, 1.5 MW Siemens turbines). The winds at this location exhibit frequent low level jet formation with significant wind speed shear with height. This site was characterized by simple flat terrain, and there was no significant wind direction shear observed (discussed later—see Figure 8). For the second experiment, the HRDL was deployed to the NREL National Wind Technology Center (NWTC) to measure the winds both upwind and downwind of a research wind turbine. This measurement campaign was part of the Turbine Wake and Inflow Characterization Study (TWICS), a joint field program involving NOAA, University of Colorado, Cooperative Institute for Research in Environmental Sciences (CIRES), Lawrence Livermore National Laboratory (LLNL) and NREL.

The HRDL performed various scan configurations to envelop the vertical and horizontal extents of the wake from the turbine. This site had fairly complex terrain with several instances of strong wind speed shear as well as wind direction shear (see Figure 9).

In both these field campaigns, the scanning strategy of the Doppler lidar was designed with the respective science goals in mind. A series of vertical and horizontal scans were performed with varying scan speeds to sample the winds with a repeat period of 15 min. The primary scanning mode for the HRDL during Lamar was the vertical slice RHI scans pointed into the mean wind. This scanning strategy was aimed at identifying low-level jets characteristics and their implications on wind turbines. The RHI scans were interspersed with some low angle and high angle PPI scans to create mean wind speed and direction profiles. Of these scans, only the low angle PPI scans (at 1°, 2° and 3°) are used in the present analysis to create a wind profile once every 15 min. Therefore, we are using a very small subset of the available data and are only able to create profiles of the required variables up to 90 m above ground level (AGL) as shown in Figure 7(a). Similarly for

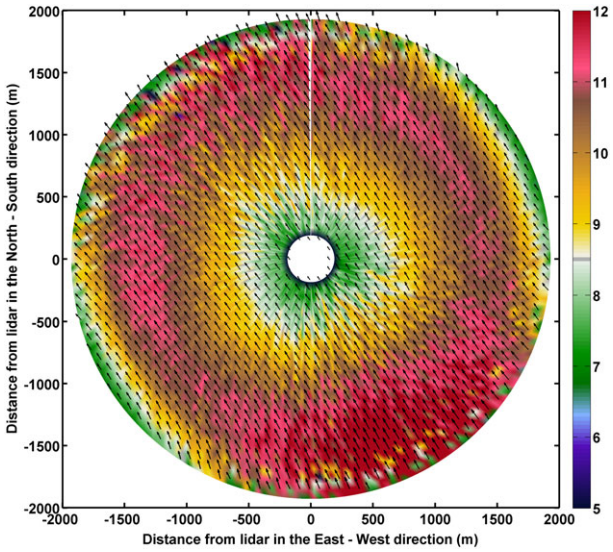

Figure 5. Example vector retrieval result from the Lamar dataset using the optimal interpolation technique. The PPI scan is at an elevation angle of 2° with the horizontal showing the presence of strong wind shear with height. The outer most measurement point is about 70 m above the lidar location (center of the plot). The colors indicate magnitude of wind speed in m s^{-1}.

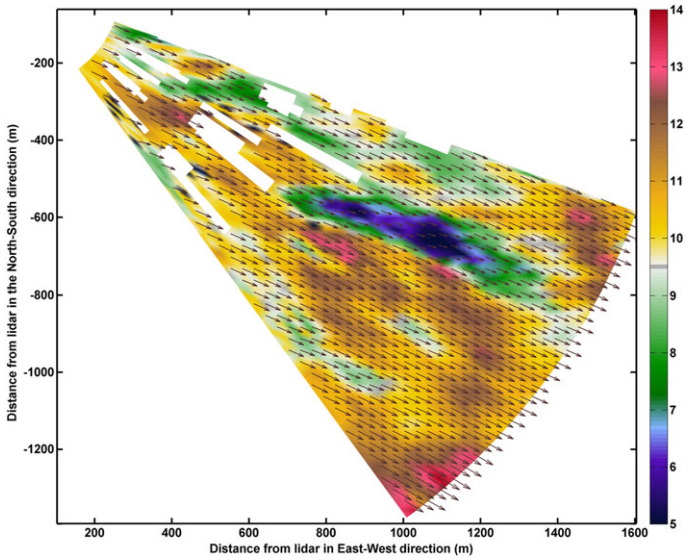

Figure 6. Example vector retrieval result from the TWICS dataset using the optimal interpolation technique. The sector scan is at an elevation angle of 2° with the horizontal. The colors indicate magnitude of wind speed in m s^{-1}. The retrieval is limited to the first 60 range-gates (~2000 m) to save computation time. The white spaces are a result of filtering out hard target returns and low SNR points.

the TWICS campaign, only the PPI sector scans of elevation angle 2°, 4° and 6° are used to retrieve the parameters required for this analysis resulting in wind profiles up to 130 m AGL (as shown in Figure 7b) every 15 min.

In order to retrieve the wind fields from the lidar data, the optimal interpolation (OI) technique[16] was used. The OI is a statistical technique which starts off with a first guess of the wind field and corrects this first guess using Bayesian formalism to estimate the maximum likelihood wind field given the first guess and the radial velocity observations. In this case, a VAD (velocity azimuth display) estimate is used as the first guess. In its present form, the OI technique is only applicable to low level PPI scans of less than 10° elevation angles.[16] Since this technique is used only for low-level PPI scans and does not make any assumptions about the homogeneity or isotropy of the wind field, it is expected to work equally well in simple or complex terrain. Previous work using this technique found that this technique provided reasonable retrievals in complex terrain (see Choukulkar *et al.*[16], Choukulkar *et al.*[17]). Example retrievals using this technique are presented in Figures 5 and 6. Figure 5 shows retrievals of wind speed and direction on a 2° elevation conical scan. As seen from the figure, the wind speed increases as one moves radially outwards from the center and then reduces towards the outer edge of the scan, which implies that the wind speed first increases with height (points away from the center are higher than points near the center of the scan because of the conical shape) and then reduces. This indicates presence of a jet maxima within the heights covered by the scan. Figure 6 shows a PPI sector scan centered on a wind turbine. The wake region behind the turbine can be identified by the cooler colors. In our analysis, care was taken to ensure we do not use the data from the wake region, by using only the beams adjacent to the wind turbine.

The retrieved wind fields were binned into vertical bins each of heights 5 m to create a vertical profile of wind speed and directions. Figure 7 shows how the data from the lidar scans was binned to create the wind speed and direction profiles. As seen from Figure 7a, data over a horizontal range of 800 m was used to create profiles of wind speed and direction for the Lamar experiment. The dashed black vertical lines indicate the start and end of the ranges used to bin the data and create the

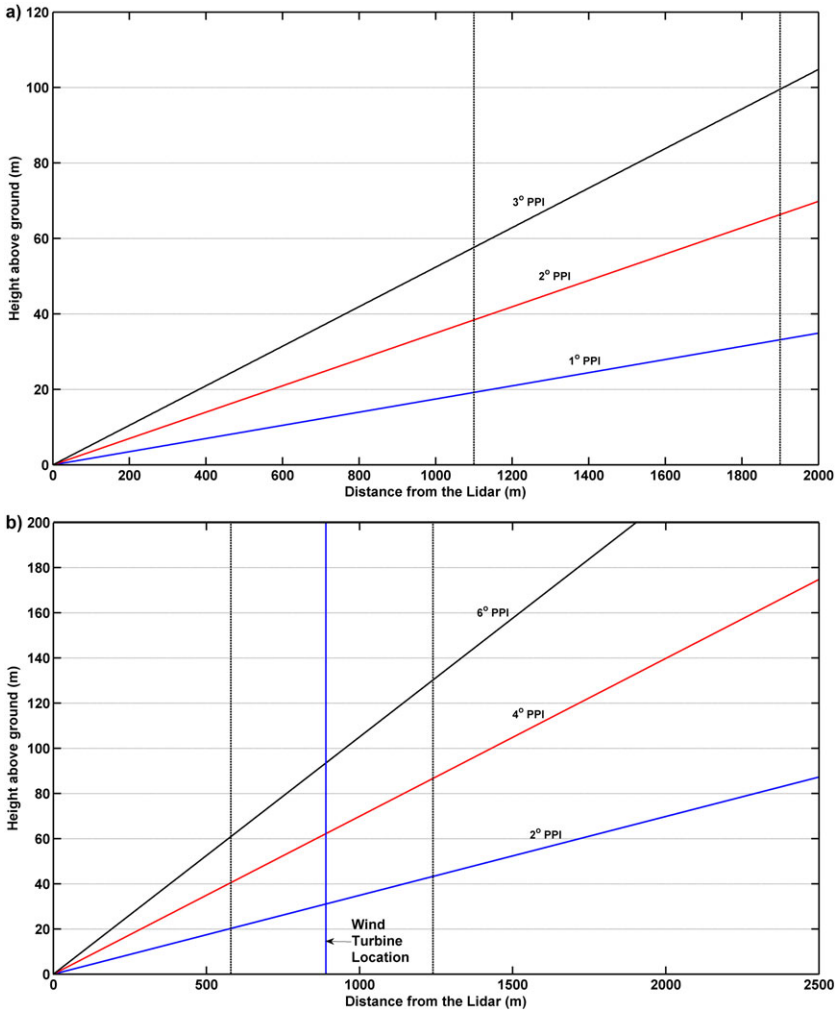

Figure 7. Schematic showing how wind profiles are created. (a) For the Lamar dataset (b) For the TWICS dataset.

profile. The choice of this range was to have a profile from 20 m above the ground and to go as high as possible. In addition, for the Lamar dataset, because of low aerosol conditions, maximum range of lidar measurements was limited to around 2000 m from the lidar. In Figure 7b we see that data over a horizontal range of 660 m is used for the TWICS experiment. In this experiment, the wind turbine location is indicated by the solid blue line. The dashed black vertical lines indicate the range of data used to create the wind profile. The selection criteria here was to include heights ranging from 20 m above the ground to 130 m above the ground so as to capture the full wind turbine rotor layer. For the TWICS dataset, additional care was taken to only use beams not contaminated by the wind turbine wake. This was done by choosing beams adjacent to the wind turbine instead of in line with it. In addition, data quality was ensured through an SNR filter which discarded data with low SNR values.

It should be noted that in this analysis we do not study the effect of turbulence intensity and variance of direction fluctuations. In order to include these variables, the temporal averaging period would have to be quite large (~2 h) given the scanning strategy and limited scans used for this analysis. Therefore only the effect of wind shear and wind direction shear is included. However, since these two parameters have the largest effect on available wind power (see Figures 2 and 3), a significant portion of the variability is captured. In addition, it is assumed that the wind turbine is always aligned such that at hub height, the axis of the rotor is parallel to the wind direction. In real-time applications, this may not always be the case, or there may be a time lag before this may be achieved. This effect is ignored in the present analysis.

The wind shear and direction shear calculated from this data is shown in Figures 8 and 9. The shear in the wind speed and direction is calculated as the difference in the value from one level to the previous level divided by the difference in height. Therefore the units are $\mathrm{m\,s^{-1}\,m^{-1}}$ for wind shear and $\mathrm{degree\,m^{-1}}$ for direction shear. The wind speed shear and wind direction shear observed during the Lamar project are shown in Figure 8. As seen from Figure 8a, there is significant wind speed shear, but very little wind direction shear (Figure 8b), a typical occurrence at this site. The choice of scanning

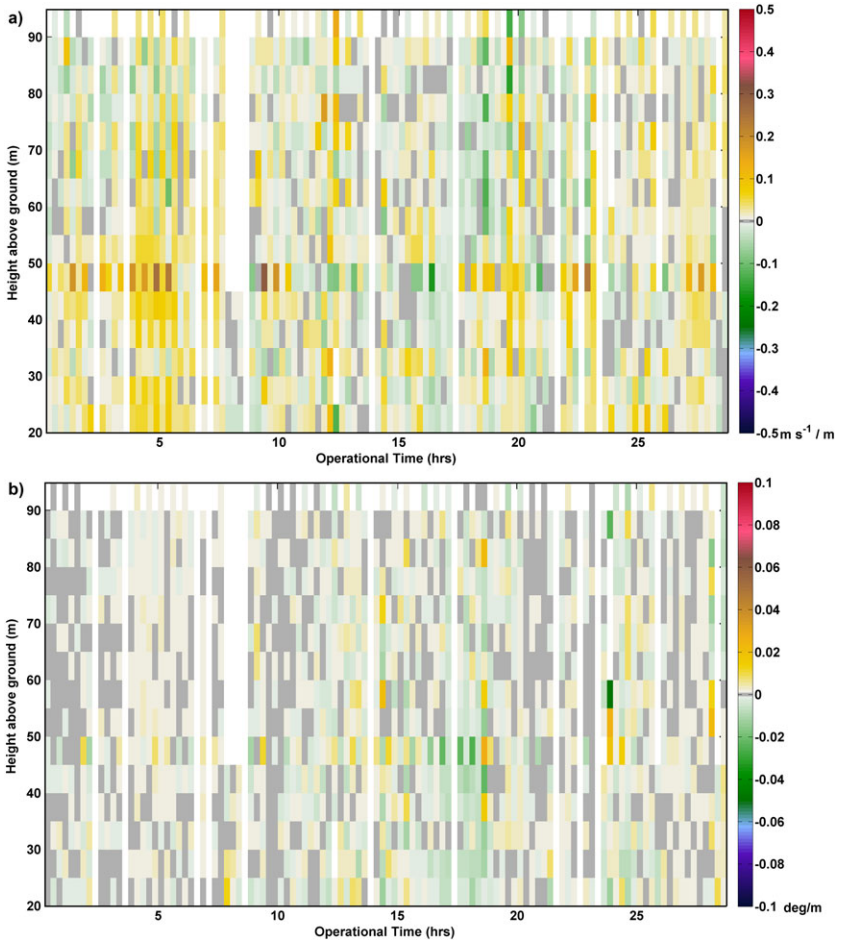

Figure 8. Wind speed and direction shear from the Lamar dataset. Each profile is created every 15 min. (a) Wind speed shear for the operational period between September 5th and 16th. (b) Wind direction shear for the operational period between September 5th and 16th. Very low wind direction shear observed.

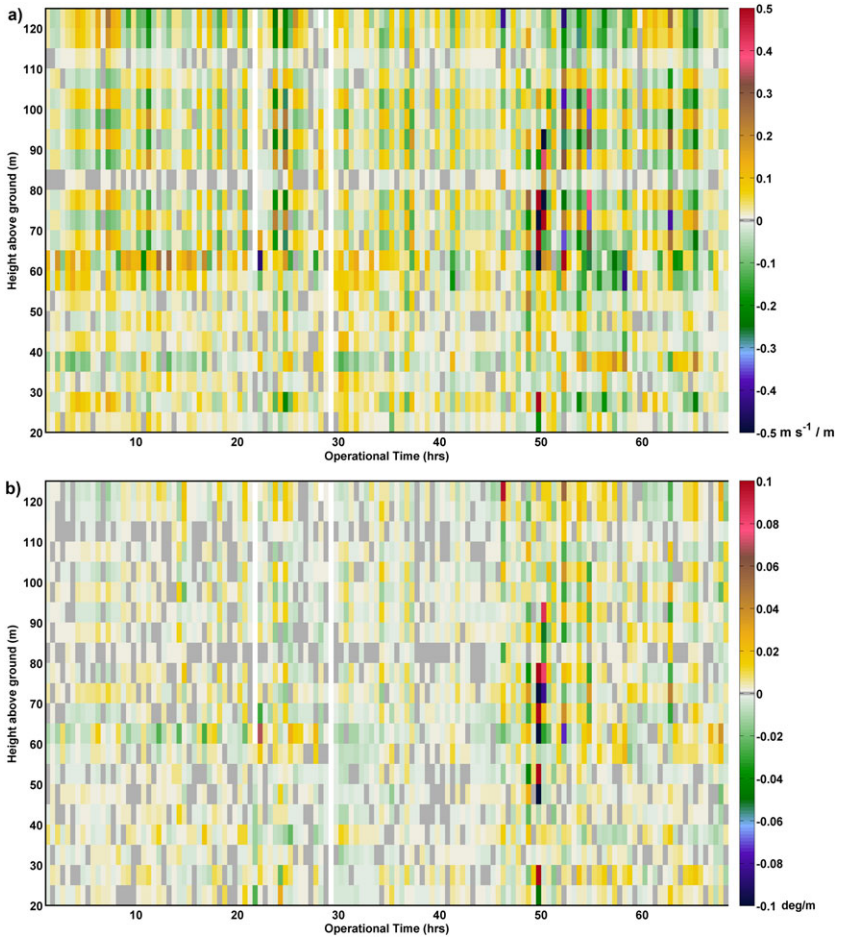

Figure 9. Wind speed and direction shear from the TWICS dataset. Each profile is created every 30 min. (a) Wind speed shear for the operational period between April 16th and 28th. (b) Wind direction shear for the operational period between April 16th and 28th. Significant wind direction shear is observed.

strategy during this experiment limits the data to only the first 90 m AGL. Whereas, the data collected during TWICS, which was conducted in complex terrain, there is substantially more wind speed and wind direction shear observed (Figure 9). In addition, the scans performed during this experiment allow estimating profiles up to 130 m AGL.

Once the wind speed and direction shear are estimated, their effect of available power can be estimated using the equivalent wind speed formulations. For the Lamar dataset, a wind turbine with hub-height 65 m and rotor diameter 52 m are assumed (modeled on the Vestas V52 wind turbine), while for the TWICS dataset a wind turbine with hub-height 80 m and rotor diameter 100 m is assumed (modeled on the Siemens 2.3 MW wind turbine). Figure 10 shows the comparison of the differences between the hub height wind speed and the equivalent wind speed calculated using the formulation proposed by Wagner *et al.*[2] and the new formulation presented in equation (7). The percentage difference is calculated as:

$$\%Difference = \frac{U\_Equivalent - U\_HubHeight}{U\_HubHeight} \times 100 \tag{9}$$

The percentage difference was calculated for the formulation by Wagner *et al.*[2] denoted by 'U_Wagner – U_Hub' (blue line) and for the new formulation denoted by 'U_NewFormula – U_Hub' (red line). It is observed that both the formulations show significant differences compared to the hub height wind speed (Figure 10). The difference between the two formulations is not significant in the Lamar data set (Figure 10a). This is expected as in the Lamar site, very low wind direction shear was observed. Therefore the two formulations provide a similar estimate of the equivalent wind speed. However, it is observed that the deviation from the hub-height wind speed is mostly negative. This is because of the nature of the wind

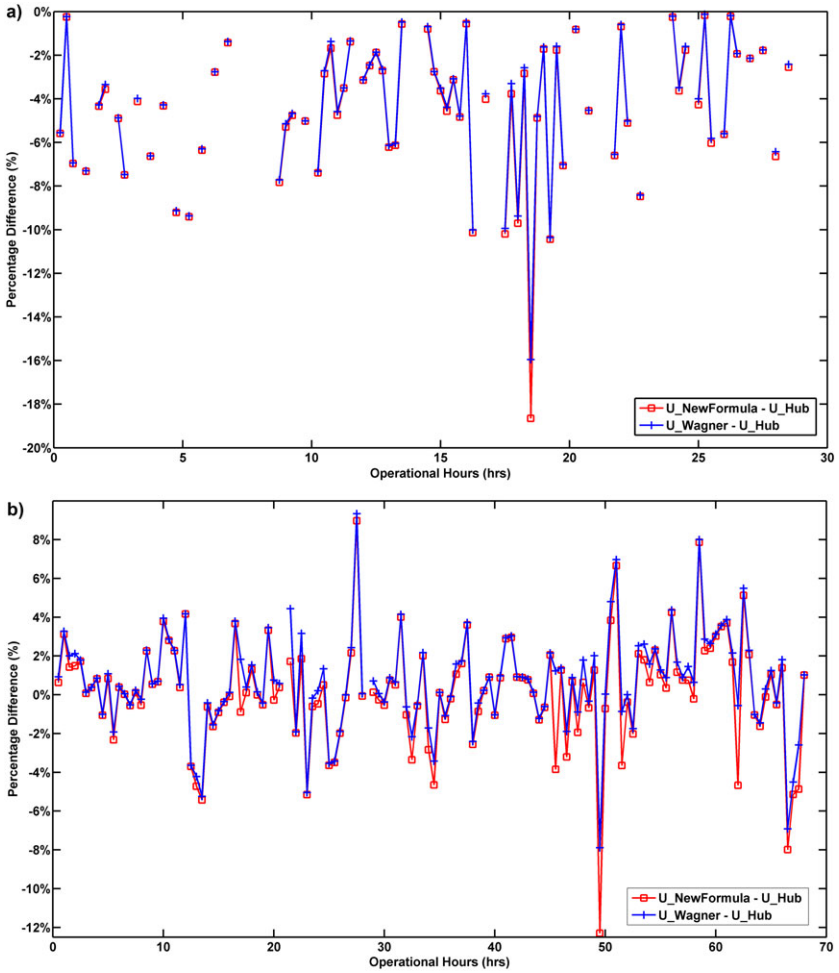

Figure 10. Percentage difference in the equivalent wind speed compared to the hub height wind speed using the new formulation [equation (7)]—red line, and the formulation by [2]—blue line. (a) Comparison for the Lamar dataset. (b) Comparison for the TWICS dataset. Note the different axis on the plots.

profile observed during this time, where the wind maxima occurred within the turbine rotor layer, which resulted in the equivalent wind speed being lower than the hub-height wind speed.

Significant differences between the two formulations are observed in the TWICS data set (Figure 10b). This is because of the presence of significant wind direction shear at this site which results in the new formulation estimating a lower equivalent wind speed value. In addition, it is observed that the two site have a considerably different wind shear profiles. In the Lamar site, wind shear results in lower equivalent wind speed values compared to hub-height wind speed (predominantly positive shear exponent values), while in the TWICS site, wind shear is seen to produce both higher and lower equivalent wind speed compared to hub-height values (both positive and negative shear exponent values).

In order to quantify the effect of wind direction shear on wind power, the percentage difference in the equivalent power estimated from Wagner *et al.*[2] formulation and the new formulation is plotted in Figure 11. The equivalent power is proportional to the cube of the respective equivalent wind speed. Therefore percentage difference is calculated as:

$$\%Difference = \frac{U\_NewFormula^3 - U\_Wagner^3}{U\_Wagner^3} \times 100 \tag{10}$$

As seen from Figures 11a and 11b, the effect of direction shear reduces the available power up to ~14%. On average the new formulation predicts the available power to be 1.3% lower than that estimated from Wagner *et al.*[2] formulation in the TWICS dataset and 0.3% lower for the Lamar dataset. Therefore it is observed that the new formulation predicts significant

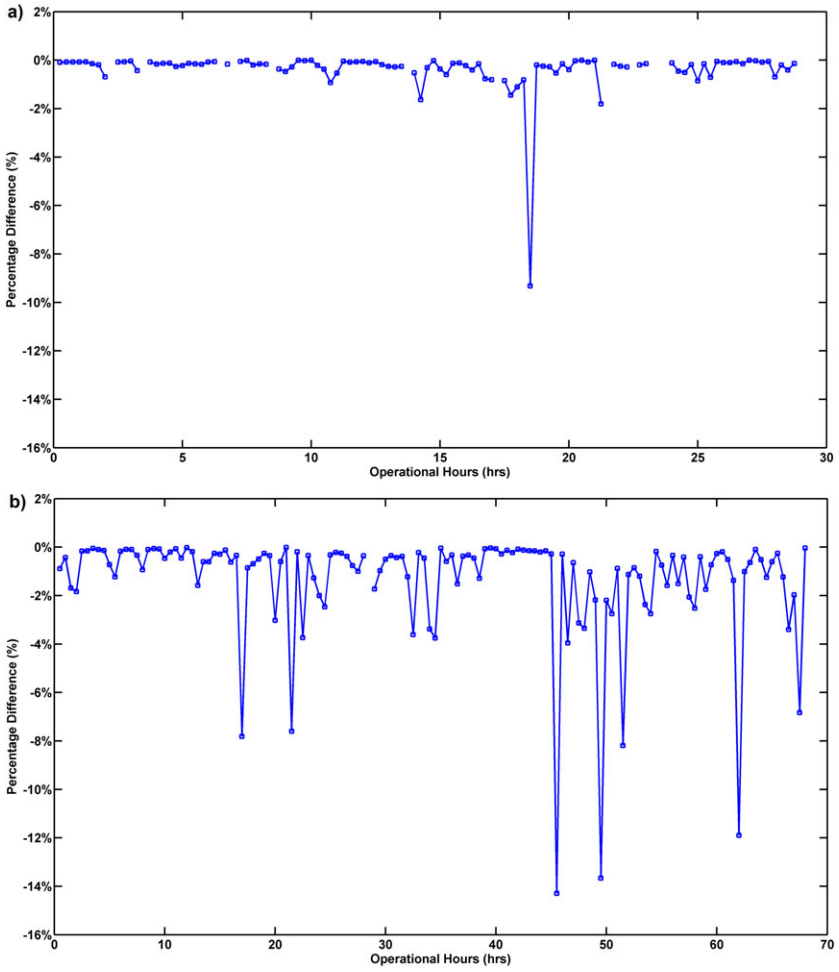

Figure 11. Percentage difference in the cubed equivalent wind speed calculated from the new formulation and from Wagner *et al.*[2]. (a) For the Lamar dataset. (b) For the TWICS dataset. Larger differences observed in the TWICS dataset because of presence of significant wind direction shear.

differences in the available power values in the presence of direction shear. This effect needs to be studied further and validated against actual power production values.

5. DISCUSSION OF RESULTS

From the results presented in the previous section, it is clear that direction shear, in addition to wind speed shear, may have a significant effect on wind power production. As seen from Figure 4, there is a significant difference in estimates of available power calculated through this formulation (equation (8)) and power production estimated from FAST. Therefore, thorough experimental evaluation of these results will be necessary to completely understand the influence of these variables on power production. Through experimental verification and simulations the theoretical formulation could be appropriately modified, if required, to estimate actual power production.

A theoretical formulation, such as the one presented here to estimate available power can be useful in several ways. This formulation can be used for wind resource assessment to arrive at an estimate of available power that accounts for not only wind shear and turbulence, but also directional shear and direction fluctuations. The formulation presented here is simple enough that it can be easily integrated into wind resource assessment performed either through measurements or through numerical model outputs. This formulation can also be used to develop optimal control strategies that produces the maximum power in the given conditions once the relationship between available energy and actual power production is well understood. For example, the results presented in this paper assume that the wind turbine yaws instantaneously to the average wind direction within the rotor swept area. However, this may not be the optimal yaw angle based on the wind

shear conditions prevalent at that time. In addition, the wind turbine will require some finite amount of time to yaw to the desired angle. Using this formulation the available power taking this lag into account could be estimated.

The results presented in the paper demonstrate the need for measurements and model outputs at several heights within the turbine rotor layer. This can be achieved quite easily through remote sensing measurements such as profiling lidars or scanning Doppler lidars. Use of scanning Doppler lidars performing PPI scans at several elevation angles (and using optimal interpolation[16] technique to retrieve wind fields) has an added advantage of capturing spatial variability, especially in complex terrain. The wind profiles used in this paper are created from just three PPI scans which result in mixing up the horizontal and vertical variations. The wind profiles could be made more representative, especially in complex terrain by using PPI scans at several elevation angles and thus reducing the horizontal averaging required to create a wind profile. In addition, understanding the spatial representativeness and sampling errors associated with creating wind profiles using different technique (VAD, Doppler Beam Swinging and OI technique) is the subject of ongoing research at NOAA Earth System Research Laboratory.

6. CONCLUSION AND FUTURE WORK

An expression for equivalent wind power has been derived that captures the effect of turbulence on available wind power content. Using this equivalent wind power equation, the effect of wind shear, turbulence intensity, direction shear and direction fluctuations on available wind power are estimated. The importance of wind speed shear has already been well documented (e.g. Wagner *et al.*[2], Wagner *et al.*[18] and Clifton *et al.*[19]). Using the new formulation, it is observed that wind direction shear also has a significant impact on the available wind power. In addition, it is shown that this equation allows estimation of the combined effect of various turbulence parameters.

Data from two field deployments, Lamar Low Level Jet Project and TWICS are used to quantify the differences in power availability estimated using the new formulation. Percentage differences in the available power calculated using the new formulation and that from Wagner *et al.*[2] is observed to be 1.3% on average in presence of wind direction shear. This observation emphasizes the importance of conducting further validation experiments to test the new formulation against measured wind turbine power output.

This result also highlights the importance of developing measurement techniques that can provide simultaneous profiles of wind speed, wind direction and their turbulent fluctuations over a wind farm area. For remote sensing instruments such as a scanning Doppler lidar, this could be a repeating stack of PPI sector scans that intersect the rotor layer at several heights. This type of scanning pattern can also be used to look upwind of a wind farm to estimate the available wind power and compare against actual power production. Performing this type of validation exercise will be essential to ascertain the accuracy of this formulation and to make improvements if necessary.

ACKNOWLEDGEMENTS

The first author would like to acknowledge the support of the Cooperative Institute for Research in Environmental Sciences (CIRES) Visiting Fellow Program during which part of this research was conducted. We thank our colleagues Neil Kelley (NREL) and Julie Lundquist (NREL/CU) for the collaboration during Lamar Low Level Jet Project and TWICS. The authors are grateful to Scott Sandberg and Ann Wieckmann for their invaluable work in deployment process and data collection.

REFERENCES

1. Sumner J, Masson C. Influence of atmospheric stability on wind turbine power performance curves. *Journal of Solar Energy Engineering* 2006; **128**: 531–538. DOI: 10.1115/1.2347714.
2. Wagner R, Antoniou I, Pedersen SM, Courtney MS, Jørgensen HE. The influence of the wind speed profile on wind turbine performance measurements. *Wind Energy* 2009; **12**: 348–362. DOI: 10.1002/we.297.
3. Wharton S, Lundquist JK. Atmospheric stability affects wind turbine power collection. *Environmental Research Letters* 2012; **7**: 014005. DOI: 10.1088/1748-9326/7/1/014005.
4. Elliot DL, Cadogan JB. Effects of wind shear and turbulence on wind turbine power curves. *European Wind Energy Conference*, Madrid, Spain, 1990, September 10–14.
5. Akhmatov V. Influence of wind direction on intense power fluctuations in large offshore wind farms in the North Sea. *Wind Engineering* 2007; **31**: 59–64. DOI: 10.1260/030952407780811384.

6. Pedersen TF. On wind turbine power performance measurement at inclined airflow. *Wind Energy* 2004; **7**: 163–176. DOI: 10.1002/we.112.
7. Kaiser K, Langreder W, Hohlen H, Højstrup J. Turbulence correction for power curves. *Wind Energy* 2007; 159–162. DOI: 10.1007/978-3-540-33866-6_28.
8. Antoniou I, Pedersen SM, Enevoldsen PB. Wind shear and uncertainties in power curve measurement and wind resources. *Wind Engineering* 2009; **33**: 449–468. DOI: 10.1260/030952409790291208.
9. Reynolds O. On the dynamical theory of incompressible viscous fluids and the determination of the criterion. *Philosophical Transactions of the Royal Society of London A* 1895; **186**: 123–164.
10. Tindal A, Johnson C, LeBlanc M, Harman K, Rareshide E, Graves AM. Site-specific adjustments to wind turbine power curves. *Proceedings of the American Wind Energy Association WINDPOWER Conference,* Houston, TX, 2008.
11. Walter K. Wind power systems in the stable nocturnal boundary layer. *PhD Thesis,* 2007.
12. Pichugina YL, Banta RM, Brewer WA, Sandberg SP, Hardesty RM. Doppler lidar-based wind-profile measurement system for offshore wind-energy and other marine boundary layer applications. *Journal of Applied Meteorology and Climatology* 2012; **51**: 327–349. DOI:10.1175/JAMC-D-11-040.1.
13. Grund CJ, Banta RM, George JL, Howell JN, Post MJ, Richter RA, Weickmann AM. High-resolution Doppler lidar for boundary-layer and cloud research. *Journal of Atmospheric and Oceanic Technology* 2001; **18**: 376–393. DOI: 10.1175/1520-0426(2001)018<0376:HRDLFB>2.0.CO;2.
14. Banta RM, Pichugina YL, Kelley ND, Hardesty RM, Brewer WA. Wind energy meteorology: insight into wind properties in the turbine-rotor layer of the atmosphere from high resolution Doppler lidar. *Bulletin of the American Meteorological Society* 2013; **94**: 883–902. DOI: 10.1175/BAMS-D-11-00057.1.
15. Kelley N, Jonkman BJ, Scott GN, Pichugina YL. Comparing pulsed Doppler lidar with sodar and direct measurements for wind assessment. *NREL/CP-500-41792*, National Renewable Energy Laboratory, Golden, CO, 2007.
16. Choukulkar A, Calhoun R, Billings B, Doyle JD. A modified optimal interpolation technique for vector retrieval for coherent Doppler LIDAR. *IEEE Geoscience and Remote Sensing Letters* 2012; **9**: 1132–1136. DOI: 10.1109/LGRS.2012.2191762
17. Choukulkar A, Calhoun R, Billings BJ, Doyle JD. Investigation of a complex nocturnal flow in Owens Valley, California using coherent Doppler lidar. *Boundary-Layer Meteorology* 2012; **144**: 359–378. DOI: 10.1007/s10546-012-9729-2.
18. Wagner R, Courtney M, Gottschall J, Lindelöw-Marsden P. Accounting for the speed shear in wind turbine power performance measurement. *Wind Energy* 2011; **14**: 993–1004. DOI: 10.1002/we.509.
19. Clifton A, Kilcher L, Lundquist J, Fleming P. Using machine learning to predict wind turbine power output. *Environmental Research Letters* 2013; **8**: 024009. DOI: 10.1088/1748-9326/8/2/024009.